Molecular Vision 2016; 22:213-223 <http://www.molvis.org/molvis/v22/213>
Received 2 September 2015 | Accepted 1 March 2016 | Published 3 March 2016

Targeting of exon VI-skipping human RGR-opsin to the plasma membrane of pigment epithelium and co-localization with terminal complement complex C5b-9

Harold Kochounian,[1] Zhaoxia Zhang,[2,5] Christine Spee,[2] David R. Hinton,[2,3,5] Henry K. W. Fong[2,4,5]

[1]Doheny Eye Institute, Los Angeles, CA; [2]Department of Ophthalmology, Keck School of Medicine of the University of Southern California, Los Angeles, CA; [3]Department of Pathology, Keck School of Medicine of the University of Southern California, Los Angeles, CA; [4]Department of Molecular Microbiology and Immunology, Keck School of Medicine of the University of Southern California, Los Angeles, CA; [5]USC Eye Institute, Keck School of Medicine of the University of Southern California, Los Angeles, CA

Purpose: Rare mutations in the human *RGR* gene lead to autosomal recessive retinitis pigmentosa or dominantly inherited peripapillary choroidal atrophy. Here, we analyze a common exon-skipping isoform of the human retinal G protein-coupled receptor opsin (RGR-d) to determine differences in subcellular targeting between RGR-d and normal RGR and possible association with abnormal traits in the human eye.

Methods: The terminal complement complex (C5b-9), vitronectin, CD46, syntaxin-4, and RGR-d were analyzed in human eye tissue from young and old donors or in cultured fetal RPE cells by means of immunofluorescent labeling and high-resolution confocal microscopy or immunohistochemical staining.

Results: We observed that RGR-d is targeted to the basolateral plasma membrane of the RPE. RGR-d, but not normal RGR, is expressed in cultured human fetal RPE cells in which the protein also trafficks to the plasma membrane. In young donors, the amount of RGR-d protein in the basolateral plasma membrane was much higher than that in the RPE cells of older subjects. In older donor eyes, the level of immunoreactive RGR-d within RPE cells was often low or undetectable, and immunostaining of RGR-d was consistently strongest in extracellular deposits in Bruch's membrane. Double immunofluorescent labeling in the basal deposits revealed significant aggregate and small punctate co-localization of RGR-d with C5b-9 and vitronectin.

Conclusions: RGR-d may escape endoplasmic reticulum-associated degradation and in contrast to full-length RGR, traffick to the basolateral plasma membrane, particularly in younger subjects. RGR-d in the plasma membrane indicates that the protein is properly folded, as misfolded membrane proteins cannot otherwise sort to the plasma membrane. The close association of extracellular RGR-d with both vitronectin and C5b-9 suggests a potential role of RGR-d-containing deposits in complement activation.

In the human eye, the RPE and Müller cells express an exon-skipping mRNA, the equivalent of which has not been found in other species [1]. This common human mRNA variant encodes a presumably nonfunctional or dysfunctional splice isoform of the RPE retinal G protein-coupled receptor (RGR OMIM 600342) opsin. RGR is a seven transmembrane-domain (TMD) visual pigment homolog that is located in the profuse smooth endoplasmic reticulum (ER) membrane of RPE cells [2-4]. The intracellular RGR opsin binds the endogenous ligand all-*trans*-retinal, which is photoisomerized stereospecifically to 11-*cis*-retinal by blue or near-ultraviolet (UV) light [5,6]. Analyses of *Rgr* $^{-/-}$ mutant mice indicate that RGR positively influences the rate of 11-*cis*-retinal synthesis both in light and in darkness after irradiation [7-10]. In the human *RGR* gene, at least two different mutations are associated with severe retinal degeneration [11]. One of these mutations (c.196A>C, p.S66R) is a rare cause of autosomal recessive retinitis pigmentosa, and another (c.824dupG, p.I276Nfs*77) leads to progressive peripapillary choroidal atrophy that is dominantly inherited [12].

The exon-skipping isoform of human RGR, referred to as RGR-d, results from an in-frame deletion of exon 6 and the complete loss of TMD6 from RGR [13]. The copy number of extraneous RGR-d mRNA is as high as 17% of the quantity of normal RGR mRNA in human RPE [14]. Immunological assays and mass spectrometric analysis independently confirm the existence of the RGR-d protein in human donor retina and RPE [14]. Unlike normal RGR, RGR-d does not localize in the ER and therefore it lacks a working ER retention signal. Instead, the protein trafficks to the basal region of RPE cells, and some quantity of RGR-d or peptide fragment thereof is released from the epithelium.

Correspondence to: Henry K. W. Fong, Department of Ophthalmology, Mudd Memorial Research Building MMR 322, 1333 San Pablo Street, Los Angeles, CA 90089; Phone: (323) 442-5559; FAX: (323) 442-6564; email: hfong@usc.edu

Deposits of extracellular RGR-d accumulate at intercapillary regions in Bruch's membrane and in all types of drusen in older donors, including patients with age-related macular degeneration (AMD). Additionally, the distribution pattern of RGR-d within the RPE-Bruch's membrane-choriocapillaris complex is dissimilar between young and old subjects [15].

To better understand trafficking and processing of RGR-d in RPE cells, we investigated the target localization of intracellular RGR-d, using high-resolution confocal microscopy. We also analyzed extracellular RGR-d to determine the potential association with other components in human Bruch's membrane. These results provide evidence that the protein-sorting path of RGR-d differs significantly from that of normal RGR and that extracellular RGR-d eventually becomes closely associated with elements of local inflammation.

METHODS

Antibodies: Commercially available monoclonal antibodies were directed against a neoepitope of the terminal complement complex C5b-9 (M0777/aE11; DAKO, Carpinteria, CA), human vitronectin (MAB1945; Chemicon, Temecula, CA), human CD46 (#555948; BD Biosciences, San Jose, CA), and syntaxin-4 (SC-101301; Santa Cruz Biotechnology, Santa Cruz, CA). The HRGR-DE7 antibody, which is directed against the identical carboxyl termini of human RGR and RGR-d, and an RGR-d-specific antibody DE21 were produced as described previously. Briefly, rabbit antisera were generated by Cocalico Biologicals, Inc. (Reamstown, PA) by immunization with synthetic peptides conjugated to keyhole limpet hemocyanin. The polyclonal antibodies were purified from antisera by affinity-binding to immobilized peptide attached to Affi-Gel 10 resin (Bio-Rad, Hercules, CA). DE21 was shown to bind recombinant RGR-d protein specifically without binding to full-length RGR. The DE21 antibody is directed against the peptide sequence (GKSGHLQVPALIAK) that corresponds to the sequence of human RGR-d at the splice junction of exons 5 and 7.

Human donor eye tissue: All experiments and procedures were conducted in compliance with applicable regulatory guidelines at the University of Southern California and the principles of human research subject protection in the Declaration of Helsinki. The Institutional Review Board of the University of Southern California approved the use of fetal eyes for culture of human RPE cells. Postmortem eyes were obtained from the Doheny Eye and Tissue Transplant Bank (Los Angeles, CA) or the National Disease Research Interchange (NDRI, Philadelphia, PA) and processed within 36 h of the time of death. Tissues for frozen sections were dissected from the central retina and processed with or without fixation. When fixation was performed, tissues were fixed with 4% paraformaldehyde in PBS (D-5652; Sigma-Aldrich, St. Louis, MO) for 4–6 h at 4 °C and then infiltrated overnight with 30% sucrose in PBS. The RPE-choroid complex was dissected from the sclera, embedded in optimum cutting temperature compound (Miles, Elkhart, IN), and frozen. The frozen tissues were sectioned with a cryostat at –20 °C to a thickness of 5–8 µm and mounted on Superfrost/Plus slides (Fisher Scientific, Pittsburgh, PA). Tissue blocks and slides were stored at −80 °C.

Immunohistochemistry: All RPE-choroid sections were treated with cold acetone for 5 min. The sections were then incubated with blocking buffer that consisted of 0.2% dodecylmaltoside, 3% (W/V) bovine serum albumin, and 5% (V/V) normal goat serum in PBS. After blocking, the sections were incubated with the primary antibody for 2 h at 22 °C and washed with 0.1% (V/V) Tween-20 in PBS. Primary antibodies were diluted with 0.2% dodecylmaltoside in PBS before immunostaining. Control slides were treated in the same manner, except that the primary antibodies were omitted from the binding buffer.

Immunohistochemical staining was detected by incubation of tissue-bound primary antibody with Impress solution (Vector Laboratories, Burlingame, CA) containing peroxidase-conjugated secondary antibody. The sections were visualized with the Vector VIP substrate (Vector Laboratories). The sections were dehydrated sequentially with increasing concentrations of ethanol, cleared with xylene, and mounted with VectaMount Permanent Mounting Medium (Vector Laboratories). Images were photographed using a Nikon Optiphot microscope with a Nikon D50 camera or the Aperio Scanscope Model CS (Leica Biosystems, Buffalo Grove, IN).

Immunofluorescence: Immunofluorescence labeling was performed by incubating tissue sections with a primary antibody and then with the fluorochrome-conjugated secondary antibody FITC-conjugated anti-rabbit immunoglobulin G (IgG) (FI-1000; Vector Laboratories) or Texas Red- (TI-2000; Vector Laboratories) or Cy3-conjugated (715-165-150; Jackson Immunoresearch Laboratories, West Grove, PA) anti mouse IgG. For double-labeling, the sections were washed with 0.1% Tween in PBS after the first primary antibody, and immunostaining was repeated with a different set of primary and secondary antibodies, as indicated in the figure legends. Negative controls were performed in parallel by omitting the primary antibodies. The sections were mounted using VECTASHIELD Mounting Medium with DAPI (Vector Laboratories) for fluorescence applications. Images were

analyzed using a PerkinElmer 6-line Spinning Disk Laser Confocal Microscope (PerkinElmer, Waltham, MA).

Human fetal RPE cell culture: Primary RPE cells were isolated from 16- to 18-week-old fetal eyes (Advanced Bioscience Resources, Inc., Alameda, CA) and cultured in Dulbecco's Modified Eagle's Medium (DMEM) with L-glutamine, penicillin/streptomycin, and 10% fetal bovine serum (FBS), as described previously [16]. RPE cells from single donors were grown to confluence in a fibronectin-coated cell culture flask or on Transwell filters (12 mm internal diameter, 0.4 µm pore size; Corning Costar, Tewksbury, MA). Polarized RPE monolayer cultures were used when transepithelial resistance was 300 Ohms·cm^2 or greater, as measured with the EVOM epithelial voltohmmeter (World Precision Instruments, Sarasota, FL).

Western blot analysis: Proteins were electrophoresed in a 12% polyacrylamide–0.1% sodium dodecyl sulfate (SDS) gel and then transferred to Immun-Blot PVDF membrane (Bio-Rad). The blots were incubated with affinity-purified primary antibody at ambient temperature and then with a secondary antibody that was conjugated to horseradish peroxidase. Immunoreactive antigens were detected by chemiluminescence using the horseradish peroxidase-based ECL (Amersham, Arlington Heights, IL) or SuperSignal West Femto (Pierce Biotechnology, Rockford, IL) substrate systems. Chemiluminescence was detected by exposure to BioMax XAR film.

Protein samples: Whole cell extracts from cultured cells, RGR-d baculovirus-transduced cells, and untreated control Sf9 cells were prepared by lysing the cells in gel-loading buffer containing 62.5 Tris-HCl, pH 6.8, 2.5% β-mercaptoethanol, and 2% SDS. The recombinant human RGR-d protein was produced using the Bac-to-Bac Baculovirus Expression System (Invitrogen, Carlsbad, CA), as described previously [13]. *Spodoptera frugiperda* (Sf9) cells were cultured in serum-free medium (Sf-900 II SFM) at 27 °C in a nonhumidified ambient air incubator. The cells were transfected with a baculovirus RGR-d expression bacmid to produce stocks of recombinant RGR-d baculovirus.

RGR and RGR-d expression vectors: To produce FLAG-RGR and FLAG-RGR-d fusion proteins, we used PCR to amplify RGR and RGR-d cDNAs from previously constructed pcDNA3-hRGR and pcDNA3-hRGR-d expression vectors, respectively [13]. The EcoRI restriction endonuclease sequences were added to both ends of the cloned fragments during PCR amplification. The sense strand primer was designed to exclude the start codons of the RGR and RGR-d pcDNA3 templates since the start codon of the pFLAG-CMV-4 vector (Sigma-Aldrich, St. Louis, MO) was to be employed. The antisense strand primer was designed to incorporate the stop codon replicated from the RGR and RGR-d pcDNA3 templates. The amplified cDNAs were then cloned into the EcoR1 cloning site of the pFLAG-CMV-4 expression vector. The sequence integrity of the new constructs, pFLAG-hRGR and pFLAG-hRGR-d, was confirmed by DNA sequencing upon comparison to published data [4].

Cell culture and DNA transfection: ARPE-19 cells (passage 10) were kindly provided by Dr. Leonard Hjelmeland (University of California Davis) [17]. The cells were cultured in DMEM/Ham's F12 (1:1) medium supplemented with L-glutamine, penicillin/streptomycin, and 10% FBS. To produce FLAG-RGR and FLAG-RGR-d as protein markers, ARPE-19 cells were transfected with the pFLAG-hRGR and pFLAG-hRGR-d DNA expression vectors using Lipofectamine 2000 Transfection Reagent, according to the manufacturer's guidelines (Invitrogen). Transfected cells were cultured initially in the presence of antibiotic G418 at 1200 µg/ml. Stable transformants were maintained in culture medium supplemented with 300 µg/ml G418.

RESULTS

Intracellular sorting of RGR-d to the RPE basolateral plasma membrane: The RGR-d isoform has a basal subcellular distribution in human RPE that differs from that of normal RGR, which tends to be concentrated in the apical portion of the cell [13]. In RPE-choroid sections from a 47-year-old male donor, immunohistochemical labeling of RGR-d with Vector VIP substrate coincided well with the basolateral surface of individual RPE cells (Figure 1A). High-resolution analysis of immunofluorescence by spinning disk confocal microscopy clearly identified labeling of the RPE basolateral plasma membrane (Figure 1B). RGR-d was observed in the RPE basolateral plasma membrane from different donors (Figure 1 and Figure 2); however, RGR-d signals within RPE cells, typically from older donors, were often weak or undetectable, whereas immunostaining of RGR-d was strong in Bruch's membrane.

Selective deposition of RGR-d in Bruch's membrane: Immunostaining of RGR-d in extracellular regions within Bruch's membrane and the intercapillary pillars indicates that the RGR-d isoform is released from the basal side of the RPE. We compared the distribution of RGR-d with another membrane protein that localizes to the basolateral plasma membrane, CD46 (membrane cofactor protein, MCP) [18-21]. We confirmed the presence of CD46 in the basolateral plasma membrane of RPE from a 64-year-old female donor (Figure 2B). Only a small amount of CD46 co-localized with RGR-d within the plasma membrane. Unlike RGR-d,

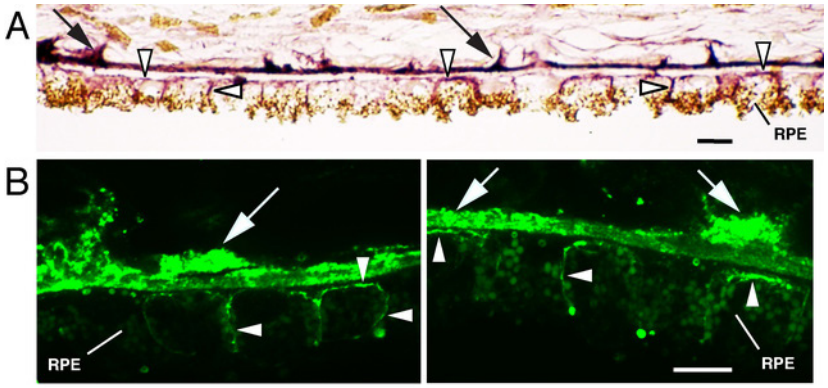

Figure 1. RGR-d in Bruch's membrane and the basolateral plasma membrane of human RPE. **A**: Immunohistochemical and (**B**) immunofluorescent labeling with RGR-d-specific DE21 antibody in Bruch's membrane (arrows) and the RPE basolateral plasma membrane (arrowheads). Strong labeling was seen in the intercapillary regions of Bruch's membrane. The sections were obtained from frozen fixed tissue and were derived from the posterior pole, including the optic disc and macula, of a 47-year-old male donor. The Vector VIP peroxidase substrate was used for immunohistochemical staining, and FITC-labeling was visualized by confocal microscopy. Scale bar, 10 µm.

immunostaining of CD46 was not predominantly localized in Bruch's membrane. Furthermore, CD46 was not found in the RGR-d-containing extracellular deposits.

RGR-d in cultured human fetal RPE cells: We analyzed the expression of RGR-d in cultured human fetal RPE cells. The cells were cultured under conditions that promote epithelial cell polarization. Whole cell extracts were probed with the RGR-specific HRGR-DE7 antibody, which is directed against the identical carboxyl terminus of human RGR and RGR-d. The immunoblot assays indicated that the *RGR* gene was expressed in the human fetal RPE cells (Figure 3A,B). We detected a highly specific protein band in each of three different donors. The single immunoreactive protein band corresponded in size most closely to the RGR-d variant, rather than the full-length RGR protein.

Intracellular localization of RGR-d in cultured human fetal RPE cells: Since polarized human fetal RPE cells appear to express predominantly the RGR-d variant, we analyzed RGR-d in the cells by immunofluorescence, using RGR-d specific antibody DE21. The results confirmed the expression of RGR-d in the cultured cells (Figure 4A). RGR-d resided mainly in the plasma membrane, along with syntaxin-4 (Figure 4B), a known plasma membrane marker in RPE cells [22]. The subcellular distribution of RGR-d and syntaxin-4 was juxtaposed, although the two proteins did not co-localize within the plasma membrane (Figure 4C). Only faint immunofluorescence of RGR-d was present in intracellular regions of these cultured cells, indicating negligible RGR-d in the ER.

Differential abundance and localization of RGR-d in the RPE-Bruch's membrane-choriocapillaris complex of young and old donors: The immunostaining pattern for RGR-d in Bruch's membrane differs between young and old donors [15]. To compare the distribution and relative amount of RGR-d in the basolateral plasma membrane of young and old RPE cells, we probed for RGR-d by immunolabeling of unfixed tissues under parallel conditions. Diffuse immunohistochemical staining results indicated that the amount of RGR-d in the RPE is significantly higher in younger tissue than in tissue

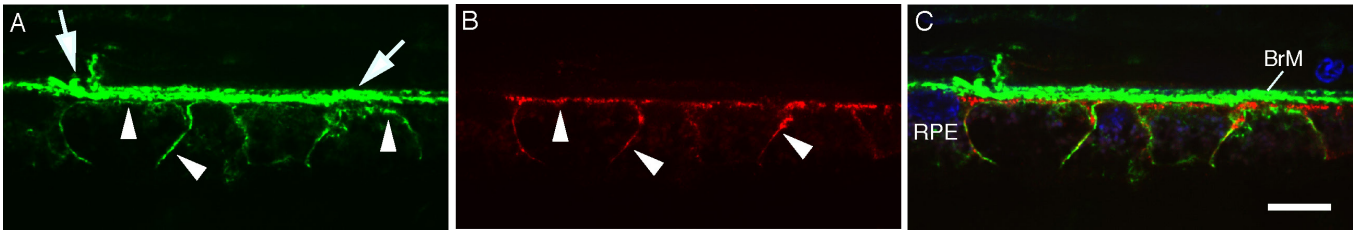

Figure 2. RGR-d and CD46 in the basolateral plasma membrane of human RPE. The RPE-choroid tissue section from a 64-year-old female donor was incubated with RGR-d-specific DE21 antibody and a monoclonal antibody directed against CD46. Double-labeling immunofluorescence with the FITC and Cy3 fluorochromes for RGR-d and CD46, respectively, was visualized by confocal microscopy. **A**: Immunofluorescent labeling of RGR-d in the RPE basolateral plasma membrane (arrowheads). Even stronger labeling was seen in Bruch's membrane (BrM; arrows). **B**: Immunofluorescent labeling of CD46 in the RPE basolateral plasma membrane (arrowheads). **C**: Localization of both RGR-d and CD46 in the basolateral plasma membrane. The merged image with DAPI counterstain showed no immunostaining of CD46 in RGR-d positive areas of Bruch's membrane. Scale bar, 10 µm.

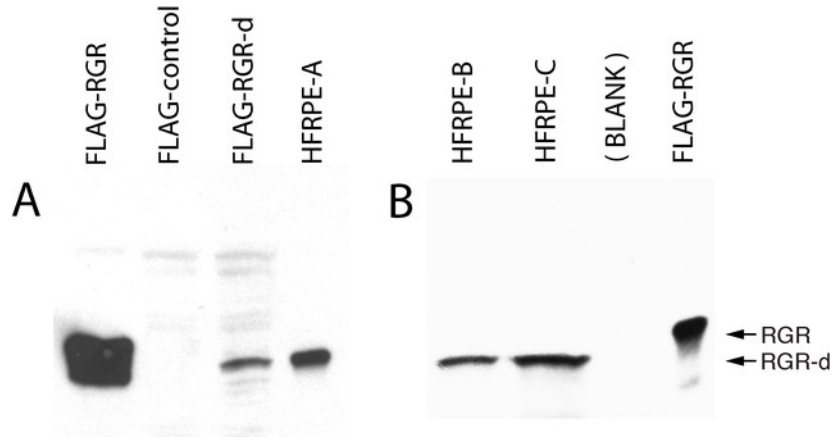

Figure 3. RGR-d protein expression in cultured human fetal RPE cells. Immunoblots of whole cell proteins were probed with the HRGR-DE7 antibody. The analysis included polarized human fetal RPE cells from different samples: (**A**) donor HFRPE-A and (**B**) donors HFRPE-B and HFRPE-C. A specific protein band that corresponds in size to RGR-d was found in each donor RPE cell. Cell extracts with FLAG-RGR and FLAG-RGR-d fusion proteins were used both for size comparison and as protein controls. pFLAG-hRGR, pFLAG-hRGR-d, and pFLAG-CMV-4 control expression vectors were transfected into ARPE-19 cells. Untreated ARPE-19 cells did not express detectable levels of endogenous RGR or RGR-d proteins.

of older donors (Figure 5A,B). Furthermore, the immunofluorescent labeling of RGR-d in young RPE is primarily in the basolateral plasma membrane and is present in the majority of RPE cells. In older donors, it is generally difficult to detect RGR-d in RPE cells. In contrast, extracellular immunolabeling of RGR-d is relatively intense in Bruch's membrane, intercapillary regions, and drusen of older donors.

Association of extracellular RGR-d with complement C5b-9 and vitronectin: To determine whether RGR-d associates with pathological features other than drusen, we compared the distribution of RGR-d with that of vitronectin and the terminal complement complex C5b-9 by means of double-label immunofluorescence. The results showed a close relationship between extracellular RGR-d and both C5b-9 (Figure 6A and Figure 7) and vitronectin (Figure 8A,B) in Bruch's membrane and small basal deposits. The spatial distribution of C5b-9 as well as vitronectin closely matched the presence of RGR-d over an extended area with a significant amount of co-localization.

DISCUSSION

RGR-d is a major isoform of RGR opsin in humans. In contrast to normal RGR, the RGR-d isoform is concentrated at the basal pole of the RPE, as determined by immunohistochemical analysis. Previous immunohistochemical staining was often diffuse and did not allow precise structural localization [13-15]. Using immunofluorescent labeling and high-resolution confocal microscopy, we have localized RGR-d to the RPE basolateral plasma membrane in addition to extracellular sites in Bruch's membrane. The localization of RGR-d in both intracellular and extracellular domains differed significantly in relation to donor age.

The targeting of RGR-d to the plasma membrane was corroborated by the analysis of human fetal RPE cells. When cultured on Transwell filters, these cells are able to form a highly differentiated polarized monolayer with high transepithelial resistance and morphological characteristics of RPE [16]. The human *RGR* gene, in addition to *RPE65*, is expressed in these cultured fetal RPE cells. Surprisingly, only the RGR-d isoform was found, and full-length RGR

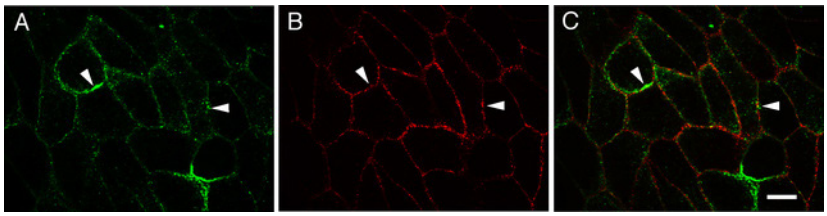

Figure 4. RGR-d and syntaxin-4 in the plasma membrane of cultured human fetal RPE cells. Polarized human fetal RPE cells from a single donor were cultured in replicate chamber wells. The cells were fixed and incubated with (**A**) DE21 and (**B**) anti-syntaxin-4 antibodies. Immunofluorescence was detected with secondary antibodies conjugated to FITC or Cy3, respectively. **C**: Both RGR-d and syntaxin-4 were detected at the cell borders (arrowheads). The merged image shows close juxtaposition but little co-localization of these two membrane proteins. Scale bar, 10 µm.

protein was not detected in the fetal RPE cells from any of several different donors. RGR-d trafficked mainly to the plasma membrane of the cultured cells, with a localization pattern similar to that of the transmembrane SNARE protein, syntaxin-4. Syntaxin-4 localizes to the basolateral plasma membrane of RPE and other epithelial cells [22,23].

The presence of RGR-d in the plasma membrane of donor RPE may indicate important protein folding behavior of the human RGR variant. The loss of exon 6 and the corresponding 38 amino acids, which encompass the entire sixth transmembrane domain of RGR, leads to the loss or masking of an ER retention signal that is functional in the full-length RGR. Despite this considerable change in structure, the altered protein is able to assume a folding conformation that allows it to escape the ER and traffick to the plasma membrane. One may expect, if any newly synthesized RGR-d possessed the properties of a misfolded membrane protein, it would be targeted for protein degradation by the ER-associated-degradation (ERAD) pathway [24-26] and would fail to locate in the plasma membrane. Interestingly, the distribution pattern of RGR-d appears to be age related. As demonstrated by the intense immunofluorescent staining of young RPE, RGR-d localizes predominantly in the basolateral plasma membrane over a range of contiguous cells. In contrast, immunostaining of RGR-d in the RPE plasma membrane is often weak or undetectable in older donors. It may be that RGR-d has a low threshold for unfolding during ER stress and other adverse conditions that are believed to disturb protein homeostasis upon aging [27-29].

One may hypothesize that RGR-d is released from human RPE as a result of membrane protein degradation via variations of the ERAD pathway or turnover at the plasma membrane. At the plasma membrane, RGR-d would perforce undergo a basal rate of protein turnover by known pathways of protein degradation [30,31]. The plasma membrane proteins that are targeted for degradation by ubiquitination are internalized by endocytosis and delivered to early endosomes. The ubiquitinated membrane proteins become packaged into intraluminal vesicles and concentrated within multivesicular bodies (MVB). MVBs then fuse with lysosomes, in which the membrane proteins and lipids are degraded. To some extent, the MVBs will fuse with the plasma membrane and release their cargo of intraluminal vesicles into the extracellular space as exosomes. Exosomes have been detected in Bruch's membrane, as described previously [32].

Although the mechanism by which RGR-d is released from the RPE is unknown, it appears that protein deposition into Bruch's membrane is a selective process. Both CD46 and RGR-d were present in the same cells, but extracellular deposits adjacent to the RPE cells contained RGR-d and not CD46 (Figure 2C). Generally, deposits of CD46 and other RPE basolateral membrane proteins, such as monocarboxylate transporter 3 [21] and bestrophin [33], are not highly abundant in human Bruch's membrane. Thus, it seems unlikely that large amounts of these basolateral membrane proteins are shed indiscriminately from the RPE.

A possible pathological significance of RGR-d-containing deposits in Bruch's membrane and drusen is

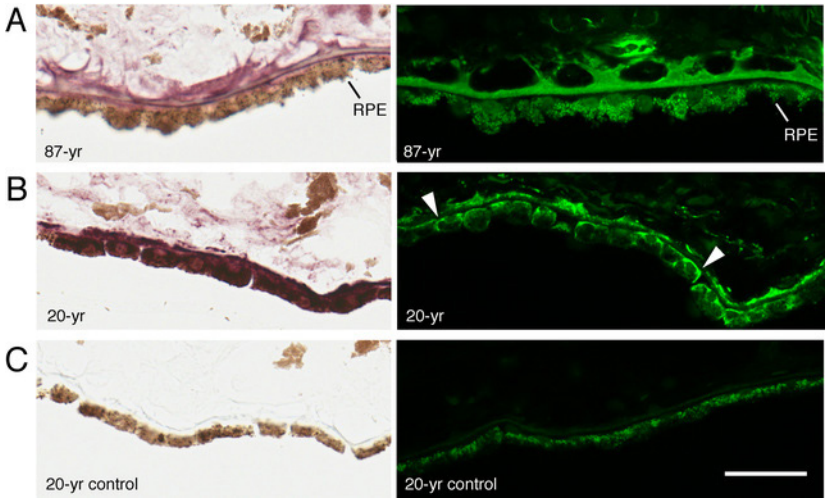

Figure 5. Differences in amount and targeting of RGR-d in the RPE and Bruch's membrane of young and old donors. All sections were from unfixed tissue and stained in parallel by immunohistochemical (left panels) and immunofluorescent (right panels) labeling of RGR-d with the DE21 antibody. **A**: RGR-d labeling in an 87-year-old female donor is predominantly in Bruch's membrane and the choriocapillaris layer but weak or absent in RPE cells. **B**: Relatively high amounts of RGR-d are present in the RPE of a young 20-year-old female donor, as indicated by strong immunohistochemical staining. Intense immunofluorescent labeling was present in the basolateral plasma membrane (arrowheads) in most RPE cells in the young donor. **C**: Negative control labeling of 20-year-old donor tissue. Scale bar, 40 µm.

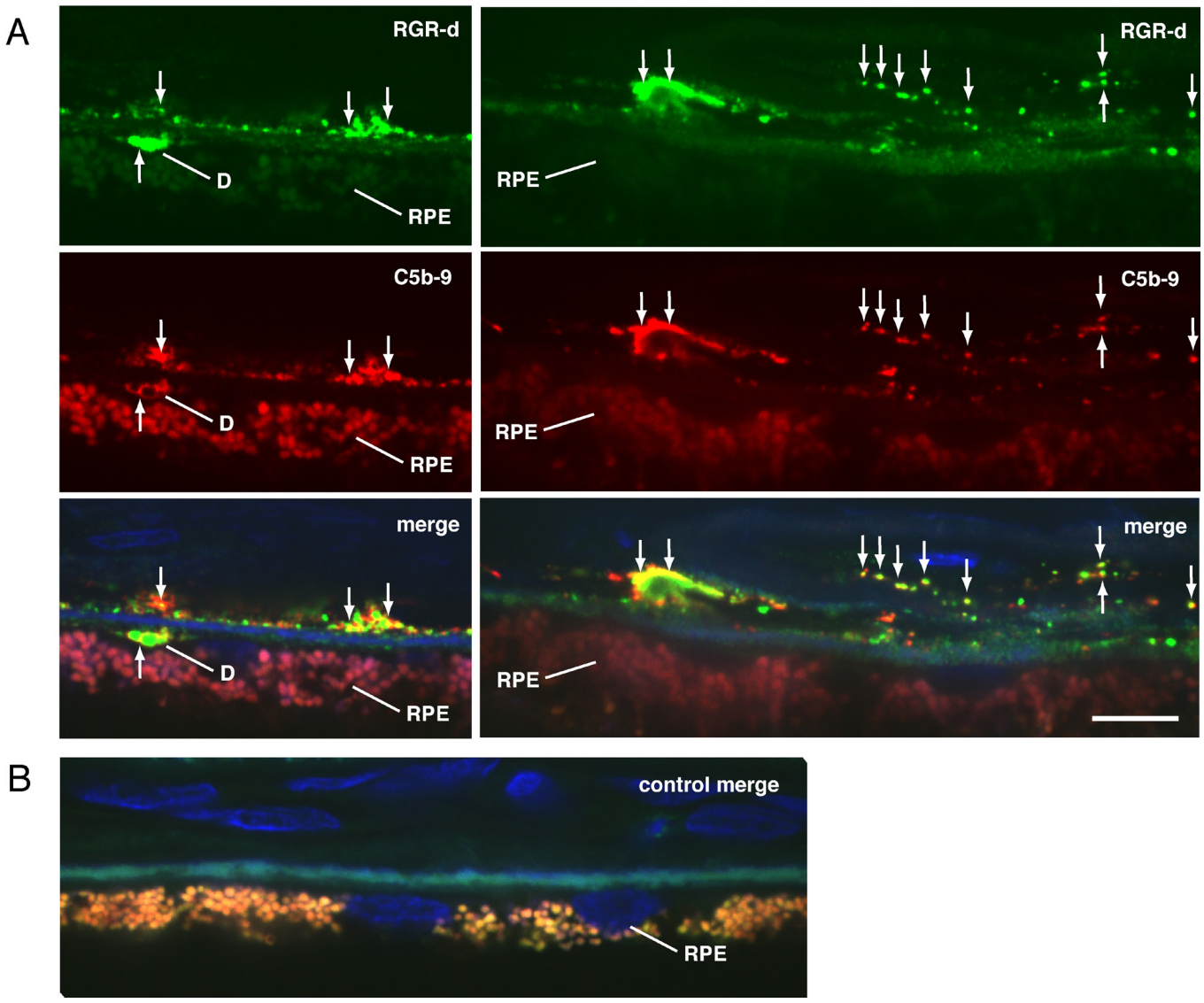

Figure 6. Close association of extracellular RGR-d and C5b-9 complement complex in Bruch's membrane. **A**: The RPE-choroid section from a 78-year-old male donor was incubated first with DE21 antibody and anti-rabbit IgG conjugated to FITC and subsequently with C5b-9 monoclonal antibody and anti-mouse IgG antibody conjugated to Texas Red. (Top panels) RGR-d aggregates, rounded bodies or speckles in Bruch's membrane, basal deposit (D), and intercapillary space are observed. (Middle panels) Specific labeling of C5b-9 in the intercapillary regions and along the walls of the capillaries coincides to a large extent with that of RGR-d. (Bottom panels) Significant co-localization of RGR-d and C5b-9 is shown with DAPI counterstain in the merged images of top and middle panels, as indicated by the arrows. **B**: Merged image of representative negative control with DAPI counterstain performed in parallel by omitting both primary antibodies. There is a complete absence of immunostaining in Bruch's membrane, choroid, intercapillary regions, and basal deposits. Autofluorescence of lipofuscin granules is visible in RPE cells. Scale bar, 10 µm.

indicated by the close association of these deposits with vitronectin and complement proteins C5b-9. Vitronectin is found in ocular drusen [34], senile plaques in Alzheimer disease [35], and other abnormal tissue [36-39]. Analyses of diseased renal tissue [40-42], human atherosclerotic arterial tissue [43], aged dermal elastic fibers [44], and diabetic choriocapillaris [45] suggest that vitronectin is significantly co-localized with the C5b-9 complex in these damaged tissues. Binding of vitronectin to C5b-9 during formation of the terminal complement complex inhibits membrane attachment, C9 polymerization, and cytolytic activity [46,47]. It is likely that vitronectin is bound to C5b-9 in Bruch's membrane and drusen, although it is also possible that vitronectin forms crosslinked protein aggregates [48,49] or is sequestered into

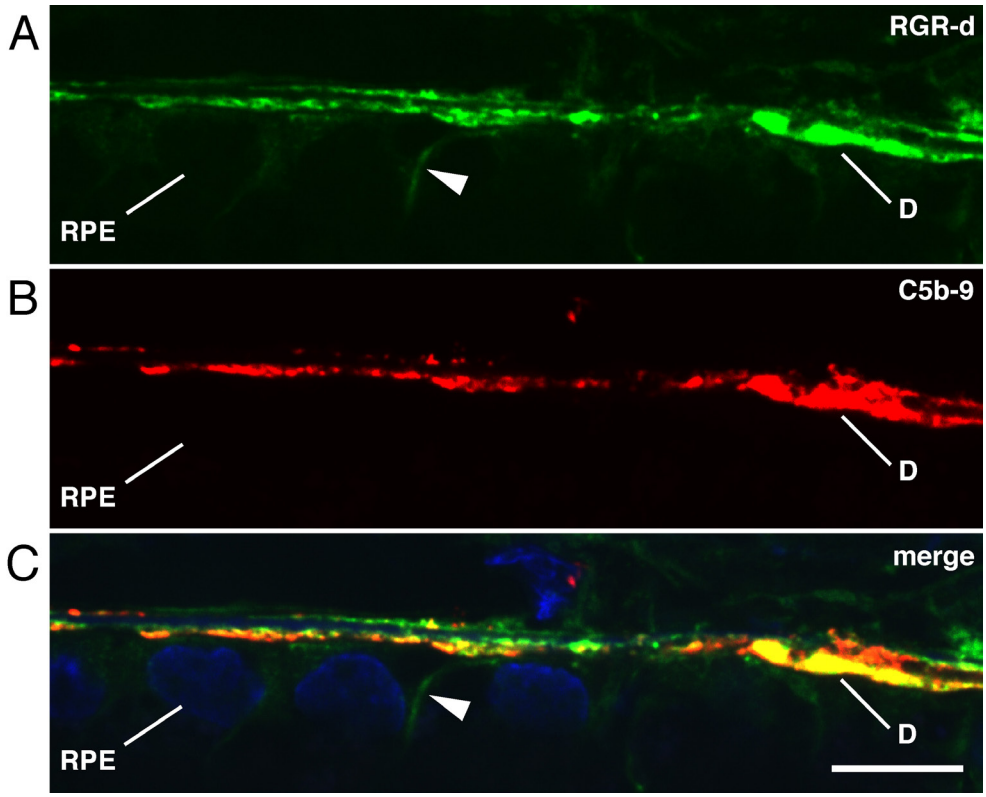

Figure 7. Localization of extracellular RGR-d and C5b-9 complement complex in basal deposits determined by double-labeling immunofluorescence in an RPE-choroid section from a 64-year-old female (same donor as in Figure 2). **A**: Basal deposits are immunoreactive with RGR-d-specific DE21 antibody and anti-rabbit IgG conjugated to FITC. **B**: Basal deposits are labeled with C5b-9 monoclonal antibody and anti-mouse IgG antibody conjugated to Cy3. **C**: The merged image with DAPI counterstain shows significant co-localization of RGR-d and C5b-9 in basal deposits (**D**). The arrowhead shows faint labeling of RGR-d in the basolateral plasma membrane. Scale bar, 10 µm.

extracelluar aggregates of a mutant protein [50]. In each case, the deposition of vitronectin correlates to regions of damaged or diseased tissue.

RGR-d is not a component or known regulator of the complement cascade, and therefore it was not expected for this epitope to co-localize with the membrane attack complex C5b-9. Thus far, few other proteins that are not part of the immune system have been reported to have widespread immunofluorescent co-localization with C5b-9 in Bruch's membrane. The close association of RGR-d with both vitronectin and C5b-9 might indicate a role in complement activation. Genetic analyses of complement genes have revealed

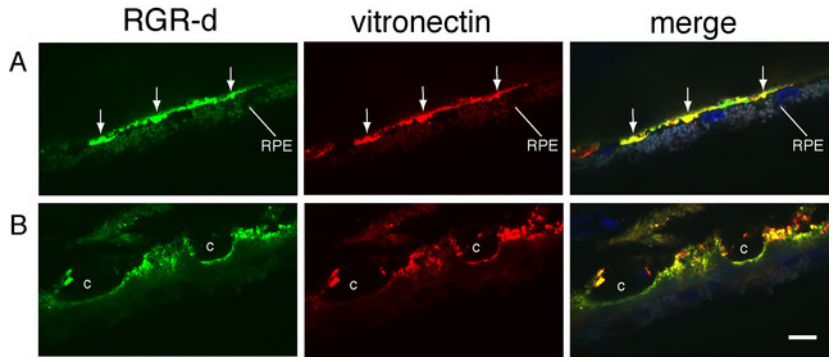

Figure 8. Association of extracellular RGR-d and vitronectin in Bruch's membrane and basal deposits. The RPE-choroid section from a 78-year-old male (same donor as in Figure 6) was incubated first with DE21 antibody and anti-rabbit IgG conjugated to FITC and subsequently with anti-vitronectin monoclonal antibody and anti-mouse IgG antibody conjugated to Cy3. **A**: Confocal image plane reveals immunoreactive basal deposits (arrows). **B**: Different confocal plane of the same field as in top panels with images that exhibit immunoreactivity in the choroid and intercapillary regions of Bruch's membrane. RGR-d immunoreactivity is detected in the basal deposits and distributed among aggregates or speckles in Bruch's membrane. Specific immunolabeling of vitronectin was also observed in each confocal image. The merged images with DAPI counterstain indicate significant co-localization of RGR-d and vitronectin in basal deposits and Bruch's membrane. Autofluorescence is visible in RPE cells. C, choroidal capillary. Scale bar, 10 µm.

that complement dysregulation is a major contributing factor in the development or progression of AMD [20,51-54]. Locally acting factors that may trigger complement activation or promote chronic inflammation in Bruch's membrane include carboxyethylpyrrole adducts [55], oxidized phospholipids and other oxidation-specific epitopes [56,57], zinc [58], bisretinoids from the RPE [59], and altered proteins in the extracellular matrix [60,61]. It is not yet known whether any of these pro-inflammatory factors are co-transported or acquired by RGR-d-containing deposits; however, it is significant that extracellular RGR-d conforms well to the natural histological distribution of the terminal complement complex. As a foreign-like component in human Bruch's membrane, erstwhile intracellular RGR-d-containing particles from the RPE may become oxidized and present neoantigens that initiate triggers of the complement surveillance system. The otherwise futile cycle of synthesis, degradation, and release of RGR-d may then work to drive long-term formation of RGR-d/complement-associated deposits and early pathogenic traits in the human eye.

ACKNOWLEDGMENTS

This work was supported in part by National Eye Institute grants P30EY03040 and R01EY01545 (DRH), R01EY08364 (HKWF), Research to Prevent Blindness, and the Gordon and Evelyn Leslie Macular Degeneration Fund (HKWF). Some of the results of this work were presented in a poster session at the 2015 Annual Meeting of The Association for Research in Vision and Ophthalmology in Denver, CO.

REFERENCES

1. Jiang M, Shen D, Tao L, Pandey S, Heller K, Fong HKW. Alternative splicing in human retinal mRNA transcripts of an opsin-related protein. Exp Eye Res 1995; 60:401-6. [PMID: 7789419].
2. Jiang M, Pandey S, Fong HKW. An opsin homologue in the retina and pigment epithelium. Invest Ophthalmol Vis Sci 1993; 34:3669-78. [PMID: 8258527].
3. Pandey S, Blanks JC, Spee C, Jiang M, Fong HKW. Cytoplasmic retinal localization of an evolutionary homolog of the visual pigments. Exp Eye Res 1994; 58:605-14. [PMID: 7925698].
4. Shen D, Jiang M, Hao W, Tao L, Salazar M, Fong HKW. A human opsin-related gene that encodes a retinaldehyde-binding protein. Biochemistry 1994; 33:13117-25. [PMID: 7947717].
5. Hao W, Fong HKW. Blue and ultraviolet light-absorbing opsin from the retinal pigment epithelium. Biochemistry 1996; 35:6251-6. [PMID: 8639565].
6. Hao W, Fong HKW. The endogenous chromophore of retinal G protein-coupled receptor opsin from the pigment epithelium. J Biol Chem 1999; 274:6085-90. [PMID: 10037690].
7. Chen P, Hao W, Rife L, Wang XP, Shen D, Chen J, Ogden T, Van Boemel GB, Wu L, Yang M, Fong HKW. A photic visual cycle of rhodopsin regeneration is dependent on Rgr. Nat Genet 2001; 28:256-60. [PMID: 11431696].
8. Maeda T, Van Hooser JP, Driessen CA, Filipek S, Janssen JJ, Palczewski K. Evaluation of the role of the retinal G protein-coupled receptor (RGR) in the vertebrate retina in vivo. J Neurochem 2003; 85:944-56. [PMID: 12716426].
9. Wenzel A, Oberhauser V, Pugh EN Jr, Lamb TD, Grimm C, Samardzija M, Fahl E, Seeliger MW, Reme CE, von Lintig J. The retinal G protein-coupled receptor (RGR) enhances isomerohydrolase activity independent of light. J Biol Chem 2005; 280:29874-84. [PMID: 15961402].
10. Radu RA, Hu J, Peng J, Bok D, Mata NL, Travis GH. Retinal pigment epithelium retinal G protein receptor-opsin mediates light-dependent translocation of all-trans-retinyl esters for synthesis of visual chromophore in retinal pigment epithelial cells. J Biol Chem 2008; 283:19730-8. [PMID: 18474598].
11. Morimura H, Saindelle-Ribeaudeau F, Berson EL, Dryja TP. Mutations in RGR, encoding a light-sensitive opsin homologue, in patients with retinitis pigmentosa. Nat Genet 1999; 23:393-4. [PMID: 10581022].
12. Leys MJ, Turner A, He H, MarBeth H, Garafalo A, Parrih R, Morris N, Tuminia SJ, Wang X. RGR gene mutation causative of peripapillary choroidal atrophy. ARVO Annual Meeting; 2014 May 4-8; Orlando, FL.
13. Fong HKW, Lin MY, Pandey S. Exon-skipping variant of RGR opsin in human retina and pigment epithelium. Exp Eye Res 2006; 83:133-40. [PMID: 16530760].
14. Lin MY, Kochounian H, Moore RE, Lee TD, Rao N, Fong HKW. Deposition of exon-skipping splice isoform of human retinal G protein-coupled receptor from retinal pigment epithelium into Bruch's membrane. Mol Vis 2007; 13:1203-14. [PMID: 17679941].
15. Kochounian H, Johnson LV, Fong HKW. Accumulation of extracellular RGR-d in Bruch's membrane and close association with drusen at intercapillary regions. Exp Eye Res 2009; 88:1129-36. [PMID: 19450444].
16. Sonoda S, Spee C, Barron E, Ryan SJ, Kannan R, Hinton DR. A protocol for the culture and differentiation of highly polarized human retinal pigment epithelial cells. Nat Protoc 2009; 4:662-73. [PMID: 19373231].
17. Dunn KC, Aotaki-Keen AE, Putkey FR, Hjelmeland LM. ARPE-19, a human retinal pigment epithelial cell line with differentiated properties. Exp Eye Res 1996; 62:155-69. [PMID: 8698076].
18. McLaughlin BJ, Fan W, Zheng JJ, Cai H, Del Priore LV, Bora NS, Kaplan HJ. Novel Role for a Complement Regulatory Protein (CD46) in Retinal Pigment Epithelial Adhesion. Invest Ophthalmol Vis Sci 2003; 44:3669-74. [PMID: 12882822].

19. Vogt SD, Barnum SR, Curcio CA, Read RW. Distribution of complement anaphylatoxin receptors and membrane-bound regulators in normal human retina. Exp Eye Res 2006; 83:834-40. [PMID: 16764856].

20. Anderson DH, Radeke MJ, Gallo NB, Chapin EA, Johnson PT, Curletti CR, Hancox LS, Hu J, Ebright JN, Malek G, Hauser MA, Rickman CB, Bok D, Hageman GS, Johnson LV. The pivotal role of the complement system in aging and age-related macular degeneration: hypothesis re-visited. Prog Retin Eye Res 2010; 29:95-112. [PMID: 19961953].

21. Vogt SD, Curcio CA, Wang L, Li C-M, McGwin G Jr, Medeiros NE, Philp NJ, Kimble JA, Read RW. Retinal pigment epithelial expression of complement regulator CD46 is altered early in the course of geographic atrophy. Exp Eye Res 2011; 93:413-23. [PMID: 21684273].

22. Low SH, Marmorstein LY, Miura M, Li L, Kudo N, Marmorstein AD, Weimbs T. Retinal pigment epithelial cells exhibit unique expression and localization of plasma membrane syntaxins which may contribute to their trafficking phenotype. J Cell Sci 2002; 115:4545-53. [PMID: 12414999].

23. Reales E, Sharma N, Low SH, Fölsch H, Weimbs T. Basolateral Sorting of Syntaxin 4 Is Dependent on Its N-terminal Domain and the AP1B Clathrin Adaptor, and Required for the Epithelial Cell Polarity. PLoS One 2011; 6:e21181-[PMID: 21698262].

24. Olzmann JA, Kopito RR, Christianson JC. The mammalian endoplasmic reticulum-associated degradation system. Cold Spring Harb Perspect Biol 2013; 5:a013185-[PMID: 23232094].

25. Ruggiano A, Foresti O, Carvalho P. ER-associated degradation: Protein quality control and beyond. J Cell Biol 2014; 204:869-79. [PMID: 24637321].

26. Zhang SX, Sanders E, Fliesler SJ, Wang JJ. Endoplasmic reticulum stress and the unfolded protein responses in retinal degeneration. Exp Eye Res 2014; 125:30-40. [PMID: 24792589].

27. Kikis EA, Gidalevitz T, Morimoto RI. Protein homeostasis in models of aging and age-related conformational disease. Adv Exp Med Biol 2010; 694:138-59. [PMID: 20886762].

28. Taylor RC, Dillin A. Aging as an event of proteostasis collapse. Cold Spring Harb Perspect Biol 2011; 3:a004440-[PMID: 21441594].

29. David DC. Aging and the aggregating proteome. Front Genet 2012; 3:247-[PMID: 23181070].

30. MacGurn JA, Hsu P-C, Emr SD. Ubiquitin and membrane protein turnover: From cradle to grave. Annu Rev Biochem 2012; 81:231-59. [PMID: 22404628].

31. Babst M. Quality control at the plasma membrane: One mechanism does not fit all. J Cell Biol 2014; 205:11-20. [PMID: 24733583].

32. Wang AL, Lukas TJ, Yuan M, Du N, Tso MO, Neufeld AH. Autophagy and exosomes in the aged retinal pigment epithelium: possible relevance to drusen formation and age-related macular degeneration. PLoS One 2009; 4:e4160-[PMID: 19129916].

33. Mullins RF, Kuehn MH, Faidley EA, Syed NA, Stone EM. Differential macular and peripheral expression of bestrophin in human eyes and its implication for Best disease. Invest Ophthalmol Vis Sci 2007; 48:3372-80. [PMID: 17591911].

34. Hageman GS, Mullins R, Russell S, Johnson L, Anderson D. Vitronectin is a constituent of ocular drusen and the vitronectin gene is expressed in human retinal pigmented epithelial cells. FASEB J 1999; 13:477-84. [PMID: 10064614].

35. Akiyama H, Kawamata T, Dedhar S, McGeer PL. Immunohistochemical localization of vitronectin, its receptor, and beta-3 integrin in Alzheimer brain tissue. J Neuroimmunol 1991; 32:19-28. [PMID: 1705945].

36. Väkevä A, Laurila P, Meri S. Regulation of complement membrane attack complex formation in myocardial infarction. Am J Pathol 1993; 143:65-75. [PMID: 7686345].

37. van Aken BE, Seiffert D, Thinnes T, Loskutoff DJ. Localization of vitronectin in the normal and atherosclerotic human vessel wall. Histochem Cell Biol 1997; 107:313-20. [PMID: 9151113].

38. Koukoulis GK, Shen J, Virtanen I, Gould VE. Vitronectin in the cirrhotic liver: an immunomarker of mature fibrosis. Hum Pathol 2001; 32:1356-62. [PMID: 11774169].

39. Okada M, Yoshioka K, Takemura T, Akano N, Aya N, Murakami K, Maki S. Immunohistochemical localization of C3d fragment of complement and S-protein (vitronectin) in normal and diseased human kidneys: association with the C5b-9 complex and vitronectin receptor. Virchows Arch A Pathol Anat Histol 1993; 422:367-73. [PMID: 8322453].

40. Falk RJ, Podack E, Dalmasso AP, Jennette JC. Localization of S protein and its relationship to the membrane attack complex of complement in renal tissue. Am J Pathol 1987; 127:182-90. [PMID: 2952015].

41. Bariety J, Hinglais N, Bhakdi S, Mandet C, Rouchon M, Kazatchkine MD. Immunohistochemical study of complement S protein (Vitronectin) in normal and diseased human kidneys: relationship to neoantigens of the C5b-9 terminal complex. Clin Exp Immunol 1989; 75:76-81. [PMID: 2467771].

42. Jansen JH, Høgåsen K, Mollnes TE. Extensive complement activation in hereditary porcine membranoproliferative glomerulonephritis type II (porcine dense deposit disease). Am J Pathol 1993; 143:1356-65. [PMID: 8238252].

43. Niculescu F, Rus HG, Vlaicu R. Immunohistochemical localization of C5b-9, S-protein, C3d and apolipoprotein B in human arterial tissues with atherosclerosis. Atherosclerosis 1987; 65:1-11. [PMID: 2955791].

44. Dahlbäck K, Löfberg H, Alumets J, Dahlbäck B. Immunohistochemical demonstration of age-related deposition of vitronectin (S-protein of complement) and terminal complement complex on dermal elastic fibers. J Invest Dermatol 1989; 92:727-33. [PMID: 2469736].

45. Gerl VB, Bohl J, Pitz S, Stoffelns B, Pfeiffer N, Bhakdi S. Extensive deposits of complement C3d and C5b-9 in the choriocapillaris of eyes of patients with diabetic retinopathy. Invest Ophthalmol Vis Sci 2002; 43:1104-8. [PMID: 11923252].

46. Su HR. S-protein/vitronectn interaction with the C5b-9 and the C8 of the complement membrane attack complex. Int Arch Allergy Immunol 1996; 110:314-7. [PMID: 8768797].

47. Podack ER, Preissner KT, Muller-Eberhard HJ. Inhibition of C9 polymerization within the SC5b-9 complex of complement by S-protein. Acta Pathol Microbiol Immunol Scand Suppl. 1984; 284:89-96. [PMID: 6587746].

48. Shin TM, Isas JM, Hsieh C-L, Kayed R, Glabe CG, Langen R, Chen J. Formation of soluble amyloid oligomers and amyloid fibrils by the multifunctional protein vitronectin. Mol Neurodegener 2008; 3:16-[PMID: 18939994].

49. Crabb JW, Miyagi M, Gu X, Shadrach K, West KA, Sakaguchi H, Kamei M, Hasan A, Yan L, Rayborn ME, Salomon RG, Hollyfield JG. Drusen proteome analysis: an approach to the etiology of age-related macular degeneration. Proc Natl Acad Sci USA 2002; 99:14682-7. [PMID: 12391305].

50. Monet-Leprêtre M, Haddad I, Baron-Menguy C, Fouillot-Panchal M, Riani M, Domenga-Denier V, Dussaule C, Cognat E, Vinh J, Joutel A. Abnormal recruitment of extracellular matrix proteins by excess Notch3ECD: a new pathomechanism in CADASIL. Brain 2013; 136:1830-45. [PMID: 23649698].

51. Bradley DT, Zipfel PF, Hughes AE. Complement in age-related macular degeneration: a focus on function. Eye (Lond) 2011; 25:683-93. [PMID: 21394116].

52. Khandhadia S, Cipriani V, Yates JRW, Lotery AJ. Age-related macular degeneration and the complement system. Immunobiology 2012; 217:127-46. [PMID: 21868123].

53. Whitcup SM, Sodhi A, Atkinson JP, Holers VM, Sinha D, Rohrer B, Dick AD. The role of the immune response in age-related macular degeneration. Int J Inflamm 2013; •••:348092-[PMID: 23762772].

54. Schramm EC, Clark SJ, Triebwasser MP, Raychaudhuri S, Seddon JM, Atkinson JP. Genetic variants in the complement system predisposing to age-related macular degeneration: A review. Mol Immunol 2014; 61:118-25. [PMID: 25034031].

55. Hollyfield JG, Bonilha VL, Rayborn ME, Yang X, Shadrach KG, Lu L, Ufret RL, Salomon RG, Perez VL. Oxidative damage-induced inflammation initiates age-related macular degeneration. Nat Med 2008; 14:194-8. [PMID: 18223656].

56. Shaw PX, Zhang L, Zhang M, Du H, Zhao L, Lee C, Grob S, Lim SL, Hughes G, Leeb J, Bedell M, Nelson MH, Lu F, Krupa M, Luo J, Ouyang H, Tu Z, Su Z, Zhu J, Wei X, Feng Z, Duan Y, Yang Z, Ferreyra H, Bartsch D-U, Kozak I, Zhang L, Lin F, Sun H, Feng H, Zhang K. Complement factor H genotypes impact risk of age-related macular degeneration by interaction with oxidized phospholipids. Proc Natl Acad Sci USA 2012; 109:13757-62. [PMID: 22875704].

57. Weismann D, Hartvigsen K, Lauer N, Bennett KL, Scholl HPN, Issa PC, Cano M, Brandstatter H, Tsimikas S, Skerka C, Superti-Furga G, Handa JT, Zipfel PF, Witztum JL, Binder CJ. Complement factor H binds malondialdehyde epitopes and protects from oxidative stress. Nature 2011; 478:76-81. [PMID: 21979047].

58. Nan R, Tetchner S, Rodriguez E, Pao P-J, Gor J, Lengyel I, Perkins SJ. Zinc-induced self-association of complement C3b and Factor H: Implications for inflammation and age-related macular degeneration. J Biol Chem 2013; 288:19197-219. [PMID: 23661701].

59. Sparrow JR. Bisretinoids of RPE lipofuscin: trigger for complement activation in age-related macular degeneration. Adv Exp Med Biol 2010; 703:63-74. [PMID: 20711707].

60. Fu L, Garland D, Yang Z, Shukla D, Rajendran A, Pearson E, Stone EM, Zhang K, Pierce EA. The R345W mutation in EFEMP1 is pathogenic and causes AMD-like deposits in mice. Hum Mol Genet 2007; 16:2411-22. [PMID: 17666404].

61. Marmorstein LY, McLaughlin PJ, Peachey NS, Sasaki T, Marmorstein AD. Formation and progression of sub-retinal pigment epithelium deposits in Efemp1 degeneration. Hum Mol Genet 2007; 16:2423-32. [PMID: 17664227].

Articles are provided courtesy of Emory University and the Zhongshan Ophthalmic Center, Sun Yat-sen University, P.R. China. The print version of this article was created on 3 March 2016. This reflects all typographical corrections and errata to the article through that date. Details of any changes may be found in the online version of the article.